COMSOL CONFERENCE 2019 BOSTON

Phase Field Modelling of Gas Migration in Bentonite-Based Barrier Material

Guanlong Guo[1], Mamadou Fall[*1]

1. Department of Civil Engineering, University of Ottawa, Ottawa, ON, Canada

*Corresponding author: 161 Colonel by, Ottawa, ON K1N 6N5, Canada. E-mail address: mfall@uottawa.ca

Abstract

Bentonite based materials (BBM) are considered as ideal buffer materials for deep geological repository (DGR) for nuclear wastes because of several desirable properties, such as low permeability, high adsorption capacity and proper swelling ability. However, gas generation and migration in the DGR may have detrimental effects on the desirable properties of the BBM. Previous experimental studies have shown that the gas migration within the BBM is characterised by the development of preferential pathways which is driven by the highly pressurised gas. This paper proposes a new coupled hydromechanical (HM) model that considers the phase field (PF) method to simulate the preferential gas flow in initially saturated and heterogeneous bentonite material.

To explicitly model the preferential pathways, the PF method is incorporated into the coupled HM framework for porous media. The governing equation for PF is implemented in COMSOL Multiphysics® by using the Coefficient Form PDE interface. In addition, the combination of a Domain ODE and a Previous Solution node is used to record the historical maximum value of elastic tensile strain energy. The coupled HM framework for porous media consists of a two-phase flow process and a deformation process. The two-phase flow process is modelled in COMSOL Multiphysics® by using two Darcy's Law interfaces (one for water flow and the other for gas flow). Moreover, the rate of volumetric strain is included in the source term of each Darcy's Law interface to account for the mechanical effects. The deformation process is modelled by the Solid Mechanics interface, in which the constitutive model for the Linear Elastic Material is modified in the Equation View to account for the damage effects caused by the PF. The average pore pressure is included in the Solid Mechanics interface by using the node of External Stress. The developed coupled HM-PF equations are solved in segregated steps by the time dependent solver.

Numerical simulation results show that the developed preferential pathway primarily passes through the area of low resistance to gas flow and fracturing, which is consistent with the physical nature and experimental results. The developed HM-PF model has been successfully implemented into COMSOL Multiphysics® and can satisfactorily capture the preferential gas flow in initially saturated bentonite.

Keywords:

Phase field; Coupled hydromechanical model; Two-phase flow; Bentonite; Nuclear waste disposal

Introduction

Bentonite based materials (BBM) are considered as ideal barrier materials for engineering barrier system of the deep geological repository (DGR) that is used for disposing high-level nuclear waste [1, 2]. This type of barrier material has several desirable properties, including low permeability, high retention capacity and self-sealing ability [1]. However, during the lifespan of DGR, a large volume of gas is expected to be generated from three basic physicochemical processes, i.e. water radiolysis, metal corrosion and biodegradation [3]. The transport of the generated gas would have negative impact on the desirable properties. Previous experimental studies showed that the dominated mechanism of gas transport in bentonite is a coupled hydromechanical (HM) behavior that is characterized by the development of preferential pathways [4]. Thus, modelling the preferential pathways from a more physical viewpoint is important for gaining a deep understanding about the gas migration process in bentonite.

In most of numerical studies, the development of preferential pathways was mainly simulated in an implicit way. To account for the effects of the developed pathways on the HM properties of the studied porous media, some nonlinear mechanical models, such as plasticity [5] and damage [6], have been used. Though these models can successfully

capture some experimentally observed behaviors, they are still limited with respect to simulating the preferential pathways from a more physical viewpoint. Currently, the widely used numerical tools to explicitly simulate fracture propagation mainly include finite element method (FEM) enriched by interface element, extended finite element method (XFEM) and discrete element method (DEM). Generally, these models suffer from either complex numerical treatments or limitations in simulating the kinking and branching of fractures [7]. In contrast, the phase field (PF) model is numerically convenient to be implemented by the standard FEM, and more capable of modeling the fracture branching and kinking [8]. In recent years, the PF method is widely used to simulate hydraulic fracturing [9, 10] and desiccation cracking [11]. Inspired by these works, this paper will incorporate the PF method into the conventional coupled HM framework, resulting in a coupled HM-PF model, to explicitly simulate the development of preferential pathways during the gas migration process in the saturated bentonite. It should be noted that the detailed model development and results analysis can be found in [7]. This paper mainly focuses on the procedures of implementing the model into COMSOL Multiphysics®.

Conceptual Coupled HM-PF Model

A conceptual coupled HM-PF model is first proposed to construct a basic framework for the numerical model to be given in the next section. The main coupling processes of the coupled HM-PF model are illustrated in Figure 1 [7].

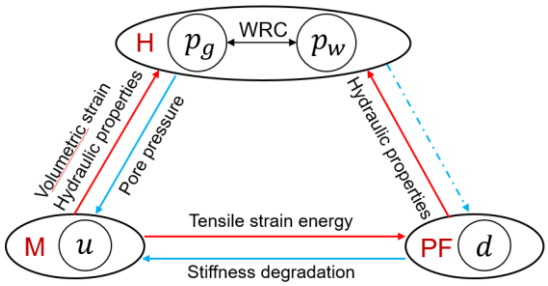

Figure 1. Couplings between different physical fields (Modified from [7]) (Note: $\boldsymbol{u}$ is displacement vector; d is phase field variable; p_w and p_w are water pressure and gas pressure, respectively; WRC denotes water retention curve; PF: Phase field; H: Hydraulic process; M: Mechanical process)

Phase Field Method

The PF method is a continuous approach to model the fracturing process in an explicit way. The sharp discontinuity is smeared by the PF variable to its surrounding area, as seen in Figure 2.

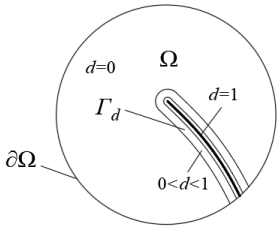

Figure 2. Smeared fracture by phase field (Note: A smeared fracture Γ_d in domain Ω with boundary $\partial\Omega$ where $d=0$, $0<d<1$, and $d=1$ denote the intact, transition and fully fractured zones, respectively)

Then, the areal integral is converted to the volume integral that can be easily implemented in the standard FEM. The functional for smearing the sharp fracture is expressed as [8]

$$A_\Gamma = \int_\Gamma dA \approx \int_\Omega \Gamma_d\left(d,\nabla d\right)dV \tag{1}$$

$$\Gamma_d\left(d,\nabla d\right) = \frac{d^2}{2l} + \frac{l}{2}\left|\nabla d\right|^2 \tag{2}$$

where Γ and Γ_d represent the sharp and the smeared fractures in the domain Ω, respectively, l is a characteristic length and d is the PF variable.

Coupled HM Process

As seen in Figure 1, the water pressure interacts with the gas pressure through the water retention curve. Then, the averaged pore pressure influences the effective stress that governs the deformation in the mechanical process. In an opposite way, the deformation changes both the mass source and the hydraulic properties in the hydraulic process. As for the coupling between the mechanical process and the phase field, the tensile elastic strain energy provides the driving force for the development of phase field. The increase of phase field variable in turn degrades the stiffness, i.e. Young's modulus. The evolution of phase field influences the HM properties, including intrinsic permeability, relative permeability and gas entry value. The direct effects of hydraulic process on the phase field are not considered in the current paper.

Numerical Model and Implementation

Hydraulic Model

The mass balance equations for water and gas can be derived from the mixture theory [12, 13]. The derived governing equation for fluid κ is expressed as

$$\underbrace{\rho_\kappa \phi\left(\frac{S_\kappa}{K_\kappa}-\frac{\partial S_e}{\partial p_c}\right)}_{S}\frac{\partial p_\kappa}{\partial t}+\nabla\cdot(\rho_\kappa \boldsymbol{v}_\kappa^D) = \underbrace{-S_\kappa \rho_\kappa \frac{\partial \varepsilon_v}{\partial t}-\rho_\kappa \phi \frac{\partial S_e}{\partial p_c}\frac{\partial p_{\kappa'}}{\partial t}}_{Q} \tag{3}$$

where κ denotes g and w for gas and water respectively, κ' denotes the other fluid different from κ, ρ_κ is the fluid density, ϕ is the porosity, S_κ is the degree of saturation, S_e is the effective degree of saturation of water, $p_c = p_g - p_w$ is the capillary pressure, K_κ is the bulk modulus of fluid κ, ε_v is the volumetric strain, $\boldsymbol{v}_\kappa^D$ is the Darcy's velocity, S is the storage term and Q is the mass source term.

The governing equation, i.e. Eq. (3), is implemented into the Darcy's Law Modulus with the Storage Node and the Mass Source Node input as the S term and the Q term in the above equation respectively. The interaction between the water pressure and the gas pressure is described by the van Genuchten model. More details of implementing the van Genuchten model in COMSOL are given in Application Libraries → Subsurface Flow Module → Two phase flow column.

The fluid flow is described by the generalized Darcy's law that is expressed as

$$\boldsymbol{v}_\kappa^D = -\frac{\boldsymbol{k}_{in} k_{r\kappa}}{\mu_\kappa}(\nabla p_\kappa - \rho_\kappa \boldsymbol{g}) \tag{4}$$

where $\boldsymbol{k}_{in}$ is the intrinsic permeability tensor, $k_{r\kappa}$ is the relative permeability, ρ_κ is the density of the fluid and μ_κ is the fluid dynamic viscosity.

To differentiate the fluid flow in the porous matrix and in the developed fracture, a transitional function is defined with respect to the phase field as

$$T(d)=\frac{1}{2}\left\{\tanh\left[\theta_t\left(d-d_{cr}\right)\right]-\tanh\left(-d_{cr}\theta_t\right)\right\} \tag{5}$$

where θ_t is a parameter controlling the slope of the transitional function, and d_{cr} is a critical value of the PF. To get an intuitive understanding, the profiles of the transitional function with different parameters are presented in Figure 3.

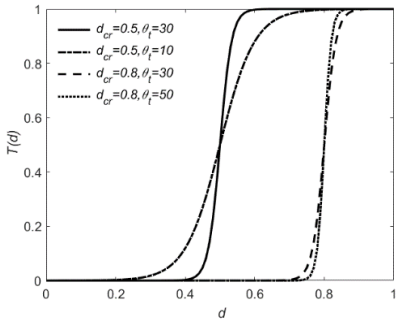

Figure 3. Profiles of transitional function with different parameters (Modified from [7])

Then, a specific hydraulic property in the transitional zone, H_t, e.g. the degree of saturation, the intrinsic and the relative permeability, can be determined by

$$H_t = T(d)H_f + \left[1-T(d)\right]H_p \tag{6}$$

where H_f and H_p are the corresponding hydraulic properties in the developed fractures and the porous matrix, respectively.

To alleviate the computational effort, the intrinsic permeability in the developed fracture is set as a constant value that is several orders of magnitude larger than the permeability in porous matrix. The relative permeability for water/gas in the porous matrix/the developed fracture can be found in [7]. The van Genuchten model [14], as expressed by Eq. (7), is used to simulate the water retention behavior of both the porous matrix and the developed fracture.

$$S_{\xi e} = \left[1+\left(\frac{p_c}{p_{\xi gev}}\right)^n\right]^{-m} \tag{7}$$

where ξ represents f and p for the fracture and the porous matrix, respectively; $p_{\xi gev}$ is the gas entry pressure, n is a shape parameter and $n = 1/(1-m)$.

In this paper, the gas entry value for the developed fracture is set as a small value to allow the gas preferentially flows through the fracture.

Mechanical Model

Neglecting the inertial and viscous forces, the momentum balance equation is expressed as [7]

$$\nabla\cdot\left[g(d)\boldsymbol{\sigma}'^{+}(\boldsymbol{\varepsilon})+\boldsymbol{\sigma}'^{-}(\boldsymbol{\varepsilon})-\bar{p}\boldsymbol{I}\right]+\rho\boldsymbol{g}=\boldsymbol{0} \tag{8}$$

where $g(d)=(1-k)(1-d)^2+k$ is the degradation function, k is a small positive value to ensure convergency, $\boldsymbol{\sigma}'^{\pm}(\boldsymbol{\varepsilon})$ is the positive or negative part of the effective stress, $\bar{p}=S_w\rho_w+S_g\rho_g$ is the average pore pressure, $\boldsymbol{I}$ is a second order identity tensor, ρ is the average density of the mixture and $\boldsymbol{g}$ is the gravitational acceleration vector.

To avoid the fracturing process caused by compressive load, the degradation function is only applied to the positive part of the effective stress tensor. The positive and negative part of the effective stress tensor, which are expressed as Eq. (9), can be determined by using the spectral decomposition technique [15, 16].

$$\boldsymbol{\sigma}'^{\pm}(\boldsymbol{\varepsilon})=\sum_{a=1}^{3}\left[\lambda\langle tr(\boldsymbol{\varepsilon})\rangle_{\pm}+2\mu\langle\varepsilon_a\rangle_{\pm}\right]\boldsymbol{n}_a\otimes\boldsymbol{n}_a \tag{9}$$

where $\langle x\rangle_{\pm}=\left(x\pm|x|\right)/2$ is the Macaulay bracket, $\{\varepsilon_a\}_{a=1,2,3}$ are the principal strains, $\{\boldsymbol{n}_a\}_{a=1,2,3}$ are the principal vectors, $tr(\boldsymbol{\varepsilon})$ is the trace of the strain tensor, $\boldsymbol{\varepsilon}$ is the strain tensor, λ and μ are the Lamé parameters.

The momentum balance equation, i.e. Eq. (8), and the mechanical constitutive model, i.e. Eq. (9), are implemented in the Structure Mechanics Modulus. The average pore pressure is accounted for by setting the Pore Pressure under the External Stress Node as $\bar{p}$ and the Biot-Willis coefficient as 1. Moreover, the principal strains and their corresponding principal vectors used in Eq. (9) have been given by the Modulus. Users can use these values, as well as Eq. (8) and (9), to define the six components of the damaged effective stress tensor. Then, the calculated stress components are used to replace the six default stress components, i.e. solid.Sl11, solid.Sl12, … solid.Sl33, under the Equation View Node of Linear Elastic Material. By far, the mechanical constitutive model is successfully implemented into COMSOL.

Phase Field Method

The governing equation for phase field is generally derived by using the variational principle of free energy minimization [16] or the microscopic force balance law [17]. These two approaches result in a same format of the governing equation for phase field. The derived governing equation for phase field is expressed as

$$(1-d)H_M^{+}-\left(d-l^2\nabla^2 d\right)=0 \tag{10}$$

where H_M^{+} is the maximum historical value of the fracture driving force, which is defined as [16]

$$H_M^{+}=\max_{\tau\in[0,t]}\left\{\left\langle\frac{\psi_0^{e+}}{\psi_{cr}}-1\right\rangle_{+}\right\} \tag{11}$$

$$\psi_0^{e+}(\boldsymbol{\varepsilon})=\frac{\lambda}{2}\langle tr(\boldsymbol{\varepsilon})\rangle_{+}^2+\mu\sum_{a=1}^{\delta}\langle\varepsilon_a\rangle_{+}^2 \tag{12}$$

$$\psi_{cr}=\frac{1}{2E}\sigma_{cr}^2 \tag{13}$$

where ψ_0^{e+} is the tensile elastic strain energy, ψ_{cr} is the critical fracture energy and σ_{cr} is the critical tensile stress.

The governing equation for phase field, i.e. Eq. (10), is implemented in a new added Physics, i.e. Coefficient Form PDE, by modifying the corresponding coefficients according to Eq. (10). The maximum historical value, H_M^{+}, can be recorded by using the Physics of Domain ODEs and DAEs and the Previous Solution Node under the Time-Dependent Solver. More details about the implementation are given in an article of COMSOL BLOG, which is titled as 'Using the Previous Solution Operator in Transient Modeling'.

Solver Settings

The developed coupled HM-PF model is a highly nonlinear model, as it consists of four governing equations and a nonlinear mechanical model. Therefore, solving the coupled model needs some appropriate settings to the Time Dependent Solver. In order to reduce the required memory and enhance the

computational efficiency, the Segregated solver is selected to solve the developed model. More details about the fully coupled and the segregated approach can be found in a COMSOL BLOG article ("Improving Convergence of Multiphysics Problems") and an article (with solution number of 1258) in Support Knowledge Base in the official website of COMSOL. The whole model is divided into three segregated steps. In each iteration, the coupled HM model, i.e. Eq. (3) and (8), is solved first based on the phase field calculated in the previous iteration. Then, the maximum historical fracture driving force, i.e. Eq. (11), is evaluated based on the displacement just calculated in the previous step. Finally, the phase field variable is determined by the calculated maximum historical fracture driving force. If the calculated results fulfill the defined convergency criterion, the solver goes to the next time step. Otherwise, the solver switches to the next iteration until the convergency criterion is fulfilled.

Simulation Results

Initial and Boundary Conditions

The meshing strategy, boundary conditions and the size of the simulated domain are presented in Figure 4. The domain of interest is the square domain that is finely meshed by the mapped element with the size of 0.25mm. The outer domain that is meshed by coarse triangular elements is added to avoid convergence issue. Note that the outer domain is only applied with the mechanical model. Boundary 5 with a length of 2 mm is prescribed as the initial fracture by setting the PF variable as 1. A constant gas flux, i.e. 2×10^{-8} kg/(m^2▪s), is applied on the initial fracture. A mass flux boundary as defined in [1] is applied on Boundary 3. The initial gas pressure (0.02 MPa) is slightly higher than the initial water pressure (0 MPa) to avoid convergence issue. Readers can refer to [7] for more details about the HM properties, initial and boundary conditions.

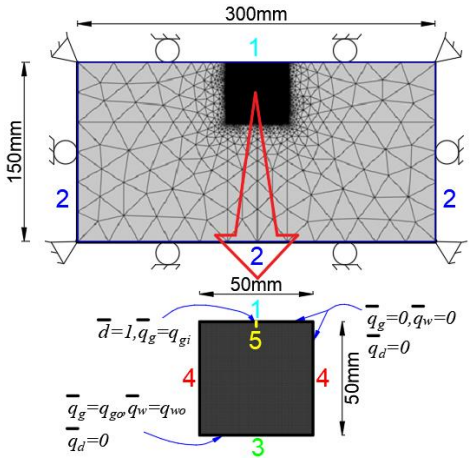

Figure 4. Meshing strategy and boundary conditions (Modified from [7]) ($\bar{q}_g$, $\bar{q}_w$, $\bar{q}_d$ are the flux boundaries for gas, water and phase field; q_{gi} and q_{go} are the values of mass flux of gas at injection and outflow boundaries, respectively; q_{wo} is the value of mass flux of water at outflow boundary)

To describe the effects of heterogeneous distribution of HM properties on the fracture patterns, a spatially auto-correlated Gaussian random field is generated by using the Cholesky decomposition technique. The random field is first created by using Matlab, and then imported into the Interpolation Function under the Node of Global Definitions. The created interpolation function can be used to define the heterogeneous HM properties that follow the log normal distribution law.

Results Analysis

Figure 5 presents the fracture trajectory (the gray area) developed during gas injection and the Gaussian random field (the contour lines). In the darker (or lighter) areas, the gas entry value, the critical tensile stress and the Young's modulus are lower (or higher), while the intrinsic permeability is higher (or lower, respectively). Therefore, the darker areas are less resistant to both the fluid flow and the fracturing process than the lighter areas. As Figure 5 shows, the fracture preferentially propagates through the areas of low resistance (darker areas) and bypass the areas of high resistance (lighter areas). This is consistent with the physical nature. Thus, the effects of heterogeneous distribution of HM properties on the fracture trajectory can be successfully captured by the developed coupled HM-PF model.

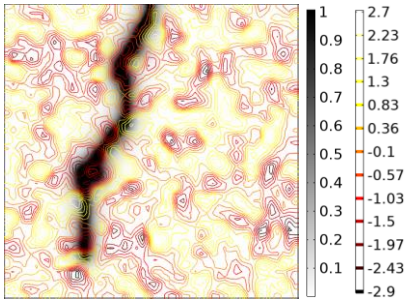

Figure 5. Fracture trajectory (Phase field) in the studied domain

Figure 6 shows the distribution of gas pressure scaled by its degree of saturation in the studied domain. The pressurized gas is localized in the developed fracture, while the pressure in the surrounding area remains close to zero. As the fracture propagates towards the bottom boundary, the opening of the developed fracture has significantly reduced the gas entry value. Therefore, the gas preferentially flows through the fracture, while leaving the porous matrix in fully saturated state. This numerical result is consistent with the experimentally observed result that the specimen kept almost saturated after gas injection test [2].

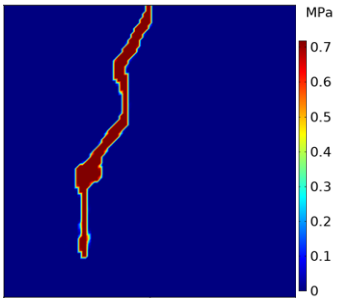

Figure 6. Distribution of gas pressure (scaled by its degree of saturation) in the studied domain

Figure 7 shows the distribution of water pressure in the studied domain. Clearly, the pore water pressure in the porous matrix surrounding the developed fracture has increased due to the compressive load exerted by the pressurized gas in the fracture. Moreover, the pore water pressure at the left side of the fracture is higher than that at the right side, as the fracture mainly propagates in the left side. Therefore, the developed coupled HM-PF model can reflect the rise and the heterogeneous distribution of water pressure during the fracturing process. This behavior is also commonly observed in experiment [2].

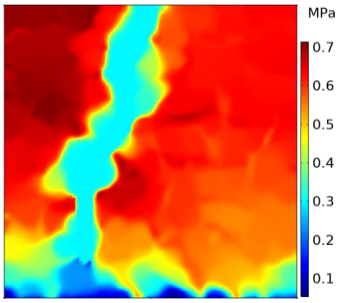

Figure 7. Distribution of water pressure in the studied domain

Conclusions

A coupled HM-PF model is successfully developed and implemented in COMSOL to simulate the preferential gas flow in bentonite barrier materials. Two Darcy's Law Modules are used to model the two-phase flow process. The Structure Mechanics Module is adopted to govern the deformation of the studied material. The governing equation for phase field is developed based on a Coefficient Form PDE, a Domain ODEs and DAEs and the Previous Solution Node. The coupled equations are solved by using the Segregated approach. The developed model has satisfactorily described some HM behaviors observed in experiments, such as the development of preferential pathways, the localized gas flow and the rise of water pressure.

References

1. Guo G, Fall M, Modelling of dilatancy-controlled gas flow in saturated bentonite with double porosity and double effective stress concepts, *Engineering Geology*, **243**: p. 253-71. (2018)

2. Graham CC, Harrington JF, Cuss RJ, Sellin P, Gas migration experiments in bentonite: implications for numerical modelling, *Mineralogical Magazine*, **76**(8): p. 3279-92. (2012)

3. Ye WM, Xu L, Chen B, Chen YG, Ye B, Cui YJ, An approach based on two-phase flow phenomenon for modeling gas migration in saturated compacted bentonite, *Engineering Geology*, **169**: p. 124-32. (2014)

4. Harrington JF, Graham CC, Cuss RJ, Norris S, Gas network development in a precompacted bentonite experiment: Evidence of generation and evolution, *Applied Clay Science*, **147**: p. 80-9. (2017)

5. Nguyen T, Le A, Simultaneous gas and water flow in a damage-susceptible bedded argillaceous rock, *Canadian Geotechnical Journal*, **52**(1): p. 18-32. (2014)

6. Fall M, Nasir O, Nguyen TS, A coupled hydro-mechanical model for simulation of gas migration in host sedimentary rocks for nuclear waste repositories, *Engineering Geology*, **176**: p. 24-44. (2014)

7. Guo G, Fall M, Modelling of preferential gas flow in heterogeneous and saturated bentonite based on phase field method, *Computers and Geotechnics*, **116**: p. 103206. (2019)

8. Miehe C, Welschinger F, Hofacker M, Thermodynamically consistent phase-field models of fracture: Variational principles and multi-field FE implementations, *International Journal for Numerical Methods in Engineering*, **83**(10): p. 1273-311. (2010)

9. Zhou S, Zhuang X, Rabczuk T, A phase-field modeling approach of fracture propagation in poroelastic media, *Engineering Geology*, **240**: p. 189-203. (2018)

10. Xia L, Yvonnet J, Ghabezloo S, Phase field modeling of hydraulic fracturing with interfacial damage in highly heterogeneous fluid-saturated porous media, *Engineering Fracture Mechanics*. (2017)

11. Cajuhi T, Sanavia L, De Lorenzis L, Phase-field modeling of fracture in variably saturated porous media, *Computational Mechanics*: p. 1-20. (2017)

12. Hu R, Chen Y, Zhou C, Modeling of coupled deformation, water flow and gas transport in soil slopes subjected to rain infiltration, *Science China Technological Sciences*, **54**(10): p. 2561. (2011)

13. Rutqvist J, Borgesson L, Chijimatsu M, Kobayashi A, Jing L, Nguyen TS, et al., Thermohydromechanics of partially saturated geological media: governing equations and formulation of four finite element models, *International Journal of Rock Mechanics and Mining Sciences*, **38**(1): p. 105-27. (2001)

14. van Genuchten MT, A Closed-Form Equation for Predicting the Hydraulic Conductivity of Unsaturated Soils, *Soil Science Society of America Journal*, **44**(5): p. 892-8. (1980)

15. Santillán D, Juanes R, Cueto-Felgueroso L, Phase-field model of hydraulic fracturing in poroelastic media: fracture propagation, arrest and branching under fluid injection and extraction, *Journal of Geophysical Research: Solid Earth*. (2018)

16. Mauthe S, Miehe C, Hydraulic fracture in poro-hydro-elastic media, *Mechanics Research Communications*, **80**: p. 69-83. (2017)

17. De Lorenzis L, McBride A, Reddy B, Phase-field modelling of fracture in single crystal plasticity, *GAMM-Mitteilungen*, **39**(1): p. 7-34. (2016)